ISSN 2288-8403(Online)

한국표면공학회지
J. Surf. Sci. Eng.
Vol.56, No.6, 2023.
https://doi.org/10.5695/JSSE.2023.56.6.386

〈Research Article〉

Reduction Kinetics of Gold Nanoparticles Synthesis via Plasma Discharge in Water

Sung-Min Kim[a], Woon-Young Lee[a], Jiyong Park[b,*], Sang-Yul Lee[c,*]

[a] Heat and Surface Technology R&D Department, Korea Institute of Industrial Technology (KITECH), Incheon 21999, Republic of Korea
[b] Advanced Joining & Additive Manufacturing R&D Department, Korea Institute of Industrial Technology (KITECH), Incheon 21999, Republic of Korea
[c] Center for Surface Technology and Applications, Department of Materials Engineering, Korea Aerospace University, Goyang 10540

(Received 03 December, 2023 ; revised 14 December, 2023 ; accepted 14 December, 2023)

Abstract

In this work, we describe the reduction kinetics of gold nanoparticles synthesized by plasma discharge in aqueous solutions with varied voltages and precursor ($HAuCl_4$) concentrations. The reduction rate of $[AuCl_4]^-$ was determined by introducing NaBr to the gold colloidal solution synthesized by plasma discharge, serving as a catalyst in the reduction process. We observed that $[AuCl_4]^-$ was completely reduced when its characteristic absorption peak at 380 nm disappeared, indicating the absence of $[AuCl_4]^-$ for ligand exchange with NaBr. The reduction rate notably increased with the rise in discharge voltage, attributable to the intensified plasma generated by ionization and excitation, which in turn accelerated the reduction kinetics. Regarding precursor concentration, a lower concentration was found to retard the reduction reaction, significantly influencing the reduction kinetics due to the presence of active H^+ and H radicals. Therefore, the production of strong plasma with high plasma density was observed to enhance the reduction kinetics, as evidenced by optical emission spectroscopy.

Keywords : Plasma process in aqueous solutions; ligand exchange reaction; reduction kinetics.

1. Introduction

In the field of nanotechnology, the synthesis of nanoparticles, particularly gold nanoparticles, has garnered considerable attention due to their unique properties and extensive applications in areas such as medicine, electronics, and catalysis [1]. Traditional methods for synthesizing these nanoparticles often involve chemical reduction processes, which can be cumbersome and environmentally hazardous [2]. Consequently, there has been a growing interest in developing alternative, more sustainable methods. Plasma in liquid solutions, or Solution Plasma Process (SPP), has emerged as a promising technique for nanoparticle synthesis [3-6]. This process involves generating plasma in a liquid medium, leading to the formation of nanoparticles through physical and chemical interactions in the plasma-liquid interface [7, 8]. The advantages of plasma discharge in solution include rapid synthesis, the absence of a requirement for chemical reducing agents, and the potential for fine control over

*Corresponding Author : Jiyong Park, Sang-Yul Lee
Korea Institute of Industrial Technology, Korea Aerospace University
E-mail: j.park@kitech.re.kr, sylee@kau.ac.kr

the nanoparticle characteristics [5-8].

Recent studies have highlighted the significance of the discharge parameters, such as voltage and precursor concentration, in determining the size, shape, and yield of the nanoparticles synthesized via plasma discharge in aqueous solutions [3, 4]. However, despite the advantages and increasing application of this method, there remains a lack of comprehensive understanding regarding the kinetics of nanoparticle formation in this context. The kinetics of nanoparticle formation is crucial for controlling the properties of the nanoparticles and optimizing the synthesis process. The present study aims to address this gap by investigating the reduction kinetics of gold nanoparticles synthesized via plasma discharge in aqueous solutions. We focus on understanding how different operational parameters, such as discharge voltage and precursor concentration, affect the rate of reduction and the final characteristics of the nanoparticles. Additionally, this study explores the role of temperature in the synthesis process, considering the significant heat generation during plasma discharge.

2. Experimental details

Chloroauric acid ($HAuCl_4 \cdot 3H_2O$, ≥99.9%, Sigma Aldrich) was added as a precursor into 200 ml of DI water to prepare a HAuCl4 solution in the range of 0.5–2.0 mM concentration. The reactor consisted of a polytetrafluoroethylene (PTFE) chamber connected to electrodes with an adjustable 0.5 mm gap between electrodes. Tungsten rods 2 mm in diameter were selected for use as electrodes owing to their high chemical and thermal resistance, good stability in shape, and high electron emissions. The electrodes are directly connected to the lines in order to apply voltage from the power sources. A unipolar power supply (JY Technologies, EnerPulse 10HV) was used under controllable discharge conditions. The voltage, were set at DC 900 V, 1000 V and 1100 V. To compare the reduction kinetics of plasma discharge in water with the thermal method, we employed a hot plate to sustain temperatures of 65℃ and 95℃ in a beaker, facilitating a direct comparison with the plasma discharge method in water. After the reduction process, a volume of 0.4 ml of NaBr-saturated aqueous solution, with a specific minimum concentration, was added to the solution.

UV-Vis spectra were recorded using a Shimadzu UV-3600 UV-Vis-NIR spectrophotometer by scanning wavelengths from 200 to 800 nm with a 10 mm absorption length. Optical emission spectroscope (OES: Ocean Optics) was also used to observe the density of plasma.

3. Results and discussion

UV-Vis spectroscopy was employed to monitor the reduction kinetics of gold nanoparticles synthesized via plasma discharge in aqueous solutions. The UV-Vis spectral peaks were systematically measured over various discharge times to determine the reduction rates. Concentrations were calculated using the Beer-Lambert law,

$$A = \sigma\_ext \times L \times C \quad (1)$$

where A represents the absorbance, σ_ext the extinction coefficient, L the path length of the cell, and C the concentration.

Typically, gold nanoparticles exhibit peak absorbance in the UV-Vis spectra around 520–550 nm. However, these peak positions can vary with changes in particle shape and size [9], making them unreliable for precise concentration measurements. In our approach, $HAuCl_4$ was utilized as

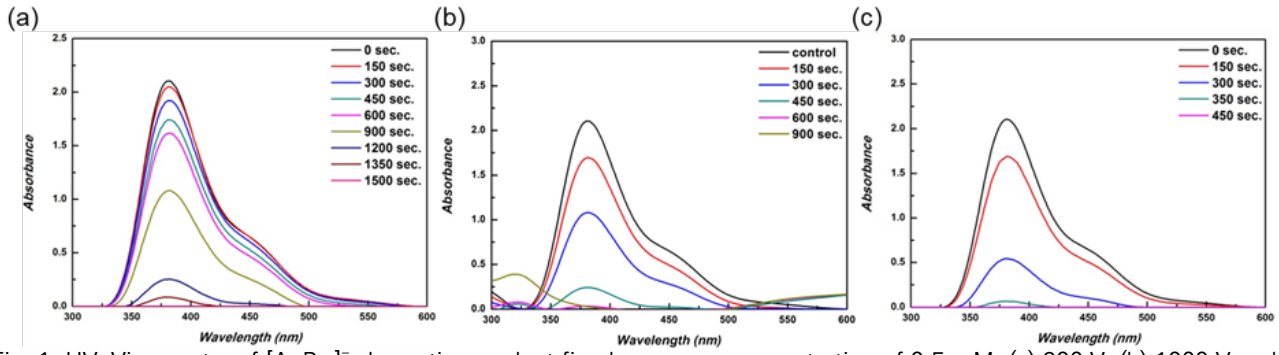

Fig. 1. UV-Vis spectra of $[AuBr_4]^-$ absorption peak at fixed precursor concentration of 0.5 mM; (a) 900 V, (b) 1000 V and (c) 1100 V

the precursor, which, upon dissolution in water, forms an electrolytic solution comprising H^+ and $[AuCl_4]^-$ ions. Addition of a sufficient quantity of Br^- ions initiates a ligand exchange reaction, transforming $[AuCl_4]^-$ into $[AuBr_4]^-$ ions [10].

Given that the path length of our cell was 10 mm, we were able to determine the extinction coefficient, as the initial precursor concentration was known. The UV-Vis spectral maximum of the $[AuBr_4]^-$ ions occurred around 380 nm. By analyzing these peaks, we quantified the concentration of the remaining precursor. Subsequently, the concentration of synthesized gold nanoparticles was deduced by subtracting the remaining precursor concentration from its initial amount. This methodology provided a more accurate and reliable measure of nanoparticle synthesis kinetics, crucial for understanding and optimizing the plasma-assisted reduction process.

Figure 1 presents UV-Vis spectral graphs depicting the relationship between various voltages and a constant precursor concentration of 0.5 mM. Notably, there was a continuous decrease in the absorbance at the signal intensity with increasing discharge time across all voltages, ultimately leading to the disappearance of these peaks. This trend indicates the progressive synthesis of gold nanoparticles, accompanied by the consumption of the precursor. The time required for the complete exhaustion of the precursor varied with voltage: at 900 V, the process took 1500 seconds, whereas at 1100 V, it was significantly quicker, requiring only 450 seconds. Figure 2 illustrates the variation in gold nanoparticle concentration over time, maintaining the same precursor concentration of 0.5 mM. The data reveal a steeper slope in the graph with increasing voltage, implying that higher voltages lead to more rapid consumption of the precursor. This observation suggests a direct correlation between the applied voltage and the rate of reduction: the higher the voltage, the faster the precursor is reduced.

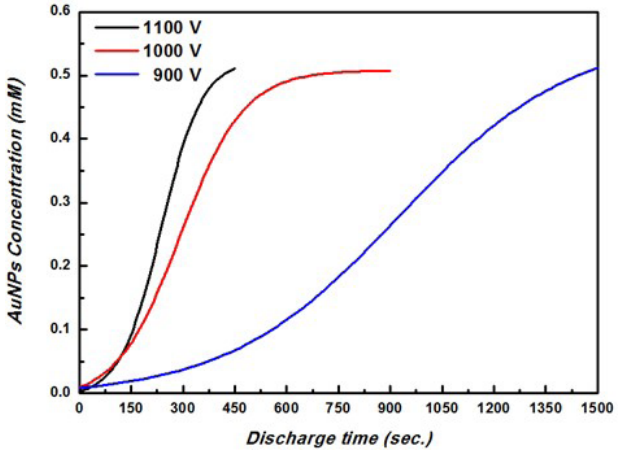

Fig. 2. Changing concentration of gold nanoparticles with increasing discharge time at fixed precursor concentration of 0.5 mM.

Figure 3 displays UV-Vis spectral graphs that show the effects of varying precursor concentrations on the absorbance at a constant voltage of 1000 V. Initially, the absorbance levels varied due to the differences in precursor concentration. In these spectra, the absorbance for the 2 mM solution (represented as (b)) was higher than

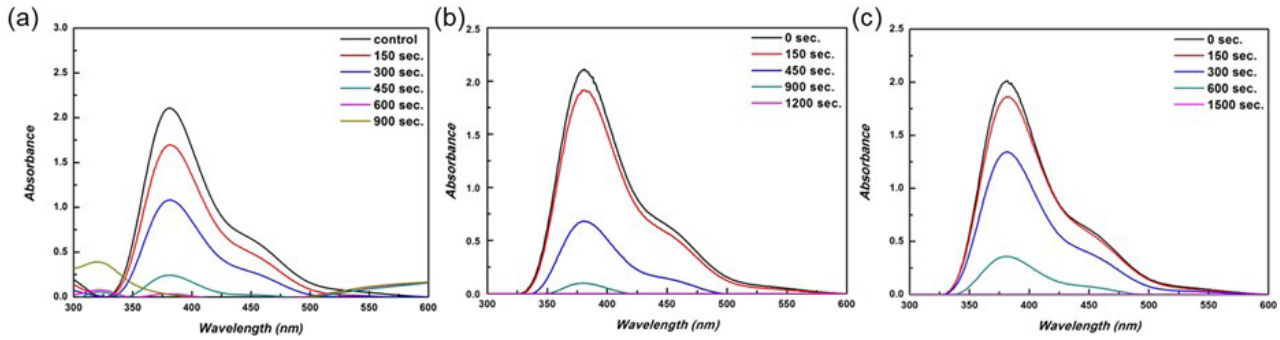

Fig. 3. UV-Vis spectra of $[AuBr_4]^-$ absorption peak at fixed voltage of 1000 V; (a) 0.5 mM, (b) 1 mM and (c) 2 mM.

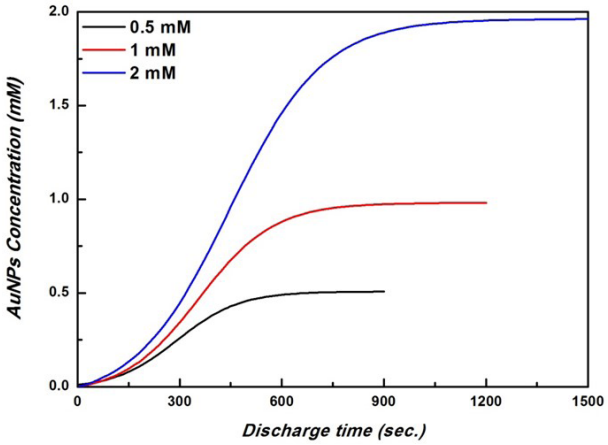

Fig. 4. Changing concentration of gold nanoparticles with increasing discharge time at fixed voltage of 1000 V.

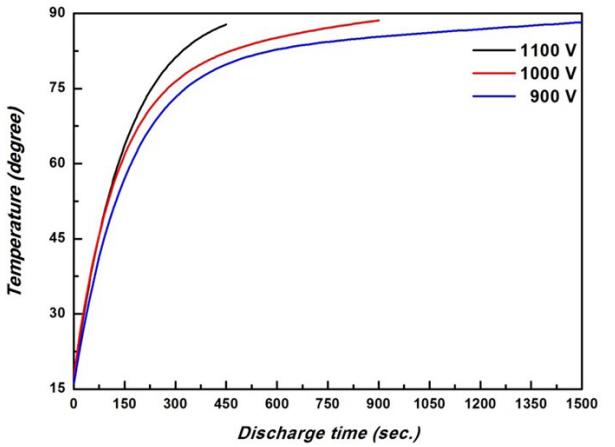

Fig. 5. Temperature with increasing discharge time depending on various voltages at fixed precursor concentration of 0.5 mM.

that of the other solutions, necessitating dilution to mitigate heavy spectral noise. As the discharge time increased, a consistent decrease in the maximum absorbance peaks was observed across all levels of precursor concentration. In Figure 4, the changes in gold nanoparticle concentration over time are presented under the same fixed voltage of 1000 V. The graph indicates a steeper increase in nanoparticle concentration with higher precursor concentrations, suggesting a more rapid reduction process under these conditions. However, it is noteworthy that the time required to completely consume the precursor increased with higher concentrations. This is attributed to the greater amount of precursor material that needs to be reduced, underscoring a key aspect of the synthesis process: the balance between the rate of reduction and the total amount of precursor available.

In the context of plasma discharge in solution, the discharge process itself generates significant heat, leading to an increase in temperature. It is crucial to understand how this temperature rise affects the rate of reduction in nanoparticle synthesis. To assess the impact of temperature on the synthesis process, separate from the effects of plasma discharge, we conducted experiments synthesizing gold nanoparticles solely through heating, without employing plasma discharge. Figure 5 presents the results, showing the temperature variation with increasing discharge time under different voltages, while maintaining a fixed precursor concentration of 0.5 mM. We observed that the temperature increased more rapidly at higher voltages. Temperature is a key factor in the synthesis of nanoparticles, and various methods employ high temperatures for the production of gold nanoparticles [11]. However, the overall temperature difference among various voltages was minimal, with all

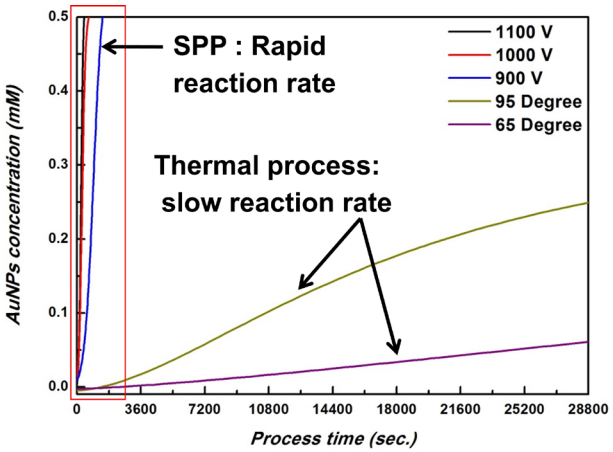

Fig. 6. Graph of comparison of reduction rate between heating and plasma discharge.

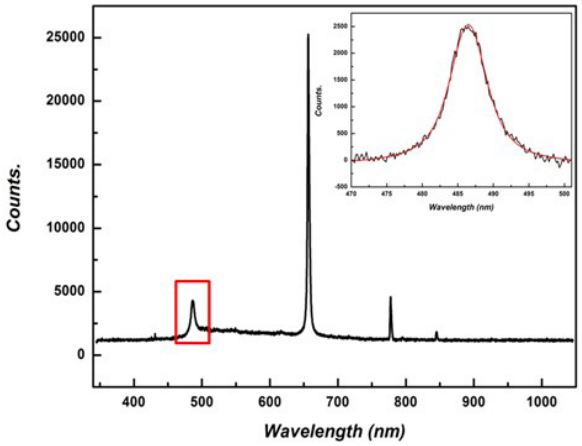

Fig. 7. OES data at 0.5 mM and 1000 V condition.

temperatures converging around 90℃.

Figure 6 presents a comparative graph illustrating the reduction rates achieved by traditional heating and plasma discharge in solution. In the heating experiments, the temperatures of the solutions were maintained at 95℃ and 65℃. The results showed that the reduction in the plasma discharge solution was completed within 1500 seconds. Conversely, the solution heated to 95℃ only achieved a 50% reduction, even after 8 hours. This stark contrast underscores the superior efficiency of plasma discharge over conventional heating in facilitating the reduction process for nanoparticle synthesis.

Reduction reaction is a chemical process characterized by the acquisition of electrons. To reduce from $[AuCl_4]^-$ to Au, enough energy and electrons should be supplied. The following reaction equation shows the process that $[AuCl_4]^-$ receiving electrons is reduced [3].

$$AuCl_4^- + e \rightarrow AuCl_2^- + 2Cl^-$$
$$AuCl_2^- + e \rightarrow 2Au^0 + 2Cl^-$$

Since the plasma discharge in solution directly provides high-energy electrons, the reaction rate is notably accelerated. The electron density within the plasma, a critical factor as the source of these electrons, was quantitatively assessed using OES. Figure 7 presents OES data recorded under conditions of 0.5 mM and 1000 V. Notably, the spectral data revealed a peak at approximately 660 nm, identified as the Hα peak, and another at around 480 nm, corresponding to the H β peak [12]. The electron density (ne) of the plasma was deduced by analyzing the Hβ peak, and this analysis was performed across all experimental conditions. To quantify the electron density in the plasma from our OES data, we utilized the Stark broadening of the Hβ emission line. The electron density was calculated based on the full width at half maximum (FWHM) of the Hβ line, using the following relation:

$$ne = f(\Delta\lambda H\beta, Te)$$

where, $\Delta\lambda H\beta$ is the measured FWHM of the Hβ emission line, Te is the electron temperature, and f represents a function that correlates these parameters to the electron density.

Figure 8 demonstrates the variation in plasma electron density with changes in voltage and precursor concentration. In Figure 8(a), a linear increase in plasma electron density is observed with escalating voltage, aligning with the principle that current is proportional to voltage. Similarly, Figure 8(b) shows an increase in electron density as the precursor concentration

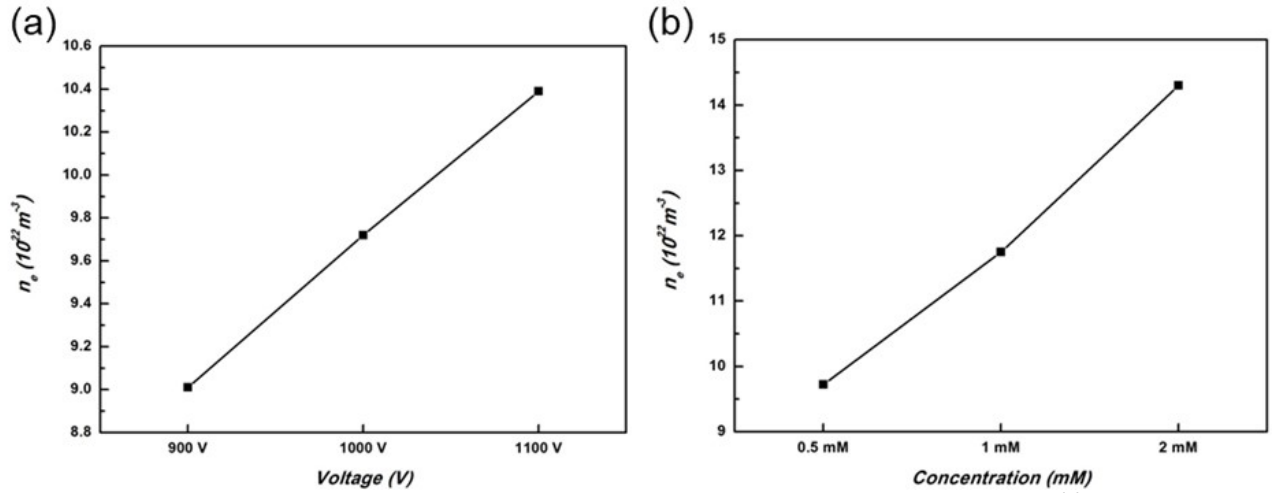

Fig. 8. Change of electron density of plasma depending on voltage and precursor concentration; (a) The condition of voltage from 900 to 1100 V and (b) The condition of precursor concentration from 0.5 to 2 mM.

rises. This can be attributed to the H^+ ions from the precursor, which reduce the electrical resistance of the solution, thereby enhancing its conductivity and contributing to plasma stability. The electron density of the plasma is found to increase with both rising voltage and precursor concentration. Correspondingly, the rate of reduction also enhances with the increasing electron density of the plasma, indicating a direct correlation between these parameters and the efficiency of the nanoparticle synthesis process.

4. Conclusions

In conclusion, the reduction rate in this study was determined by monitoring the change in the absorbance peak of $[AuBr_4]^-$ at 380 nm, resulting from the ligand exchange reaction. A comparative analysis between the plasma discharge in solution and the traditional heating method was conducted to evaluate the effect of temperature on the reduction process. It was observed that plasma discharge, which inherently raises the temperature of the solution, was a more efficient method for reduction compared to heating. Furthermore, the reduction rate was found to be directly proportional to the plasma density, which increased with the voltage. Additionally, an increase in the precursor concentration also led to a higher reduction rate, likely due to the augmented concentration of H^+ ions in the solution.

Acknowledgement

This research was supported by the Korea Institute of Industrial Technology (JE230027).

References

[1] T. Patil, R. Gambhir, A. Vibhute, A.P. Tiwari, Gold nanoparticles: synthesis methods, functionalization and Biological Applications, Journal of Cluster Science, 34 (2023) 705-725.

[2] P.G. Jamkhande, N.W. Ghule, A.H. Bamer, M.G. Kalaskar, Metal nanoparticles synthesis: An overview on methods of preparation, advantages and disadvantages, and applications, Journal of Drug Delivery Science and Technology, 53 (2019) 101174.

[3] S.M. Kim, G.S. Kim, S.Y. Lee, Effects of PVP and KCl concentrations on the synthesis of gold nanoparticles using a solution plasma processing, Materials Letters, 62 (2008) 4354-4356.

[4] S.M. Kim, S.Y. Lee, The plasma-induced formation of silver nanocrystals in aqueous solution and their catalytic

activity for oxygen reduction, Nanotechnology, 29 (2018).

[5] Y.K. Heo, S.M. Kim, S.Y. Lee, Effects of discharge duration on the size and shape of gold nanoparticles synthesized using solution plasma processing, Physica Scripta, T139 (2010).

[6] Y.G. Jo, S.M. Kim, J.W. Kim, S.Y. Lee, Composition-tuned porous Pd-Ag bimetallic dendrites for the enhancement of ethanol oxidation reactions, Journal of Alloys and Compounds, 688 (2016) 447-453.

[7] S.M. Kim, Y.G. Jo, S.Y. Lee, The composition-controlled synthesis of Pt-Ag bimetallic nanochains for catalytic methanol oxidation, Electrochimica Acta, 174 (2015) 1244-1252.

[8] S.M. Kim, Y.K. Heo, K.T. Bae, Y.T. Oh, M.H. Lee, S.Y. Lee, Formation of nitrogen-doped onion-like carbon as catalyst support for enhanced oxygen reduction activity and durability, Carbon, 101 (2016) 420-430.

[9] V. Amendola, M. Meneghetti, Size Evaluation of Gold Nanoparticles by UV-vis Spectroscopy, The Journal of Physical Chemistry C, 113 (2009) 4277-4285.

[10] A.J. Canumalla, N. Al-Zamil, M. Phillips, A.A. Isab, C.F. Shaw, Redox and ligand exchange reactions of potential gold(I) and gold(III)-cyanide metabolites under biomimetic conditions, Journal of Inorganic Biochemistry, 85 (2001) 67-76.

[11] M. Bechelany, X. Maeder, J. Riesterer, J. Hankache, D. Lerose, S. Christiansen, J. Michler, L. Philippe, Synthesis mechanisms of organized gold nanoparticles: influence of annealing temperature and atmosphere, Crystal Growth & Design, 10 (2010) 587-596.

[12] M.A. Gigosos, M.A. González, V. Cardeñoso, Computer simulated Balmer-alpha, -beta and -gamma Stark line profiles for non-equilibrium plasmas diagnostics, Spectrochimica Acta Part B, 58 (2003) 1489-1504.